Journal of Electronic Imaging

JElectronicImaging.org

Hyperspectral imaging applied to demolition waste recycling: innovative approach for product quality control

Silvia Serranti
Roberta Palmieri
Giuseppe Bonifazi

SPIE. IS&T imaging.org

Hyperspectral imaging applied to demolition waste recycling: innovative approach for product quality control

Silvia Serranti,* Roberta Palmieri, and Giuseppe Bonifazi
Sapienza–University of Rome, Faculty of Civil and Industrial Engineering, Department of Chemical Engineering, Materials, and Environment, Via Eudossiana 18, Rome 00184, Italy

Abstract. Hyperspectral imaging (HSI) based sensing devices were utilized to develop nondestructive, rapid, and low cost analytical strategies finalized to detect and characterize materials constituting demolition waste. In detail, HSI was applied for quality control of high-grade recycled aggregates obtained from end-of-life concrete. The described HSI quality control approach is based on the utilization of a platform working in the near-infrared range (1000–1700 nm). The acquired hyperspectral images were analyzed by applying different chemometric methods: principal component analysis for data exploration and partial least-square-discriminant analysis to build classification models. Results showed that it is possible to recognize the recycled aggregates from different contaminants (e.g., brick, gypsum, plastic, wood, foam, and so on), allowing the quality control of the recycled flow stream. [DOI: 10.1117/1.JEI.24.4.043003]

Keywords: concrete aggregates; demolition waste; recycling; hyperspectral imaging; quality control.

Paper 15178P received Mar. 10, 2015; accepted for publication Jun. 19, 2015; published online Jul. 23, 2015.

1 Introduction

Demolition waste (DW) recycling is an interesting option to reduce the exploitation of the natural resources and the environmental impacts (CO_2 emissions) associated with the construction sector.[1] Indeed, the improvement of the environmental world condition depends on adopting recycling strategies finalized to the production of marketable clean aggregates. Aggregates can be considered "clean" when pollutants (such as brick, glass, paper, cardboard, plastic, wood, gypsum, and so on), usually present in a DW stream, are absent or under the limits required by the market. In order to set up effective sorting and/or a quality control system, material characterization is a crucial step and end-of-life (EOL) concrete identification is important to make DW conversion into useful secondary raw materials easier. In this perspective, the development of strategies for automatic recognition of recovered products and the possibility to utilize efficient, reliable, and low cost sensing technologies that are able to perform detection/control actions during all recycling steps, are very important.

Exploring the possibility to classify a DW stream by optical sensors in order to recognize concrete aggregates and unwanted polluting materials is the main aim of this study. The developed recognition/classification method is based on the utilization of hyperspectral imaging (HSI) sensing devices working in the near-infrared (NIR) range (1000–1700 nm). The HSI system is composed of an integrated hardware and software architecture able to digitally capture and handle spectra, as they proceed along a predefined alignment on a surface sample that is properly energized.[2,3]

HSI is a type of multivariate imaging. A typical multivariate image is an image of I rows and J columns measured for K variables. The variables can be K wavelengths.[4] Therefore, data collected through a hyperspectral sensor generate a three-dimensional (3-D) dataset, the "hypercube," characterized by two spatial dimensions and one spectral dimension. The wavelength bands in hyperspectral images are typically in an equally spaced sequence; as a consequence, a full spectrum is obtained for each pixel. Each pixel in a hyperspectral image can be analyzed when the system is given spectral information about samples. According to the different investigated wavelengths and the spectral sensitivity of the device, several physical–chemical features, linked to their spectral attributes, can be collected. The HSI approach can, thus represent a powerful solution for characterization, classification, and quality control of different materials in several applications fields. For these reasons, NIR-HSI has rapidly emerged and has quickly grown in recent years, including in the solid waste sectors: glass recycling,[5] automotive shredder residue characterization (i.e., fluff),[6] bottom ashes resulting from municipal solid waste incinerators,[7] compost products quality control,[8,9] different polymers identification,[10–13] construction and DW recycling,[14,15] and so on.

2 Materials and Methods

2.1 *Analyzed Demolition Waste Samples*

Investigated samples came from the demolition of two towers located in Groningen (The Netherlands).[16] The samples are composed of concrete aggregates obtained by ADR processing carried out at TUDelft (Delft, The Netherlands) and selected typologies of unwanted contaminants: brick, foam, wood, plastic, and gypsum (Fig. 1).

The sample set was utilized to perform both a preliminary test and a second experimental test. The preliminary test was performed with the specific aim to find the best classification strategy for aggregate recognition, whereas the second experimental test was carried out in order to identify and classify each typology of material, which are aggregates and the single different pollutants.

*Address all correspondence to: Silvia Serranti, E-mail: silvia.serranti@uniroma1.it

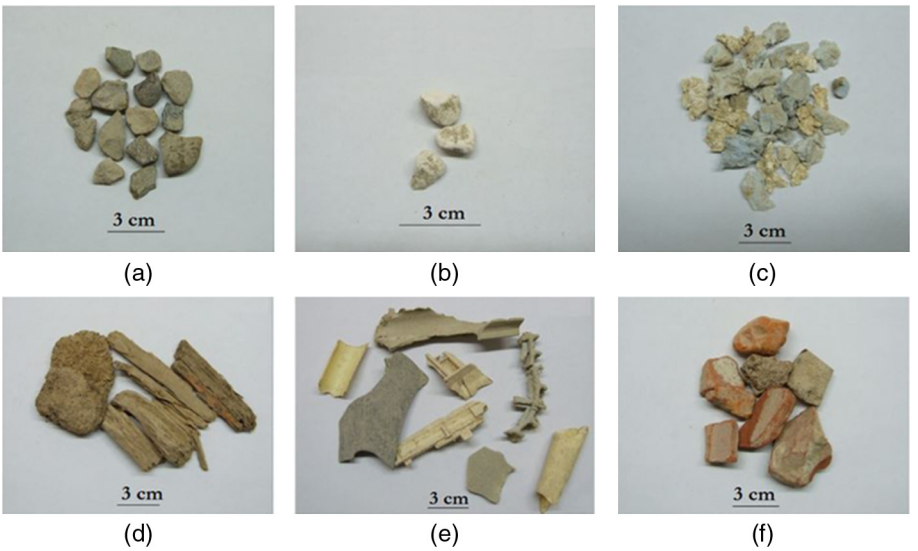

Fig. 1 Aggregates and contaminants utilized to perform recognition/classification procedures finalized to fully identify both (a) aggregates and the different polluting materials: (b) gypsum, (c) foam, (d) wood, (e) plastic, and (f) brick.

The same images were thus analyzed for both tests: for each kind of material, some particles were selected and acquired. HIS-based classifications were performed adopting three different acquisition procedures, as described in the following:

1. A training set was generated to be utilized for the subsequent classification stage. In detail, a set of 16 particles clearly identified as brick (2 particles), aggregates (3 particles), wood (1 particle), gypsum (3 particles), foam (3 particles), and plastic (4 particles) was used in order to build the classification model.
2. A validation set composed of the same particles utilized for training was then created to perform validation/classification: the classification model was preliminarily validated by applying it to the same particles, but with a different topological assessment in the acquired image.
3. The classification model was then applied to an external image dataset containing aggregate and contaminant materials different from those already acquired.

A simplified scheme showing the adopted procedure is reported in Fig. 2.

In the preliminary test, a two class model was built in order to recognize aggregates to recycle from contaminants, whereas in the second experimental test, a six class model was implemented in order to classify the aggregates and all the different classes of contaminants in each image.

The preliminary test was performed as a simplified case study in order to understand material spectral behavior and to explore the possibility to recognize contaminants and

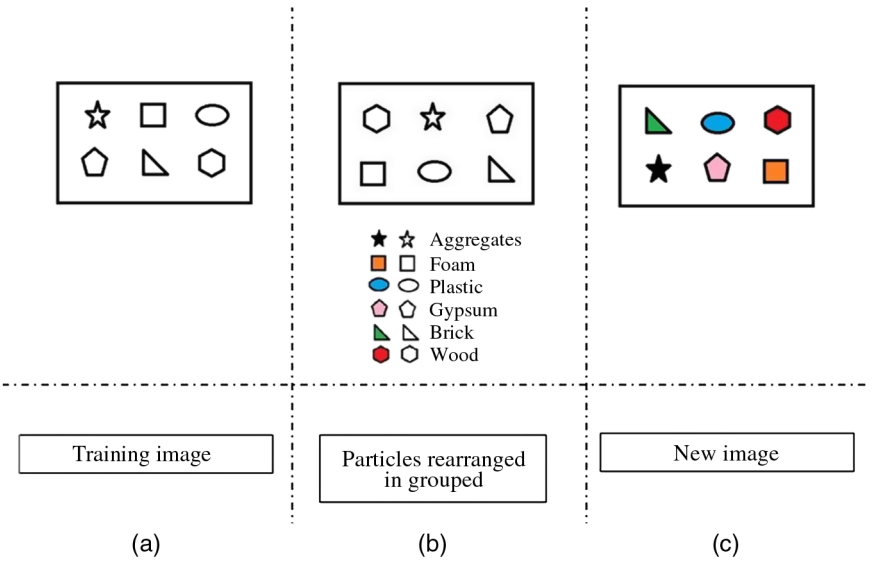

Fig. 2 Pictorial example of the procedure utilized to perform contaminants and aggregates recognition/classification: (a) image used for training, (b) same particles as presented in the training image, topologically rearranged and utilized for model validation, (c) new image constituted by different particles of the same contaminant and aggregate products.

aggregates. The second experimental test was realized as a more complex case, where each object in a sample set, representative of a typical DW stream treated in a recycling plant, was fully identified. This second strategy can be adopted in order to monitor the efficiency of the previous separation systems.

In Table 1, a synthetic explanation of the applied procedure is shown.

2.2 *Hyperspectral Imaging Equipment*

HSI acquisitions and analyses were carried out at the laboratory for particles and particulate solids characterization of Department of Chemical Engineering, Materials, and Environment (Sapienza –University of Rome) in Latina, Italy. The acquisition platform utilized to acquire the spectra of the DW samples was designed by DV srl (Padova, Italy) as a system able to simulate the behavior of a material flowstream in a real industrial plant.

In Fig. 3, the HSI based station used to acquire NIR images is shown. The detection architecture is constituted by a conveyor belt (width = 26 cm and length = 160 cm) with adjustable speed, an NIR Spectral Camera (Specim, Finland) equipped with an ImSpector N17E imaging spectrograph working in the NIR spectral field (1000–1700 nm) coupled with a Te-cooled InGaAs photodiode array sensor (320 × 240 pixels). The energizing source consists of an anodized aluminum cylinder with additional aluminum coating inside. It creates the right illumination on the sample to avoid specular reflections or dark areas. Five halogen lamps produce an intense and continuous spectrum signal from 380 to 2500 nm, especially in IR range which is adequate for spectral sensor sensitivity. The spectral sampling/pixel was 2.6 nm. The device works as a push-broom type line scan camera and acquires contiguous spectral information for each pixel in the line. Acquisitions are controlled by a PC unit equipped with a specialized acquisition/preprocessing software: Spectral Scanner v.2.3, allowing the management of different units, to perform acquisition, to collect spectra, and to perform preliminary spectra analysis.

2.3 *Data Acquisition*

Hyperspectral images were acquired in the 880–1720 nm wavelength range, with a spectral resolution of 7 nm, for a total of 121 wavelengths. The spectrometer was coupled to a 15 mm lens. The images were acquired by scanning the investigated samples line by line: their width was 320 pixels, while the number of frames was variable according to the sample size.

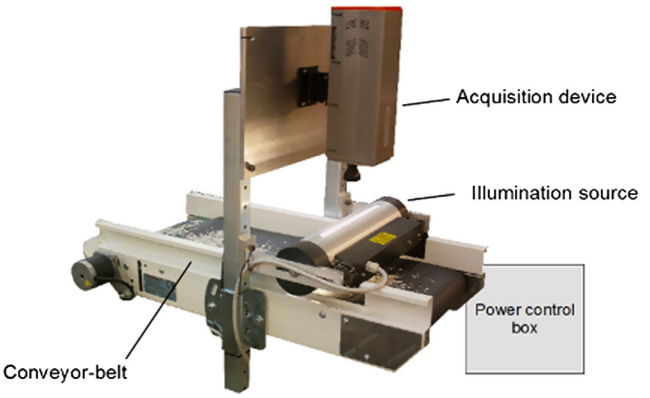

Fig. 3 The hyperspectral imaging (HSI) based station used to acquire near-infrared (NIR) images.

Before the acquisition phase, system calibration was carried out by recording an image for black and another for white. The black image (B) was acquired to remove the effect of the dark current of the camera sensor, turning off the light source and covering the camera lens with its cap. The white reference image (W) was acquired adopting a standard white ceramic tile under the same conditions as the raw image. Image correction was performed by adopting the following equation:

$$I = [I_0 - B]/[W - B], \tag{1}$$

where I is the corrected hyperspectral image in a unit of relative reflectance (%). I_0 is the original hyperspectral image, B is the black reference image (~0%), and W is the white reference image (~99.9%). All the corrected images were then used to perform the HIS based analysis.

3 Spectral Data Analysis

Spectral data were analyzed using the PLS_Toolbox (Version 7.8, Eigenvector Research, Inc., Wenatchee, Washington) running under MATLAB® (Version 7.5, The Mathworks,

Table 1 Synthetic recap of the applied strategies used to perform contaminants and aggregates recognition/classification.

Experimental setup	Aim	PLSDA classification model	Applied algorithms
Preliminary test			
Two classes were set on the training image: contaminants and aggregates. Other two acquisitions were then used as validation images.	This preliminary test was performed in order to recognize aggregates from contaminants, and not to classify every class of contaminants	Two-classes model	SNV normalization and mean center
Second experimental test			
The same images used for the preliminary set were used in order to build a six classes model: foam, brick, gypsum, wood, plastic, and aggregates were thus recognized/classified.	The second experimental test was realized as a real case, being representative of a typical DW stream treated in a recycling plant with the specific aim to identify and classify each material	Six classes model	Detrend, SNV normalization and mean center

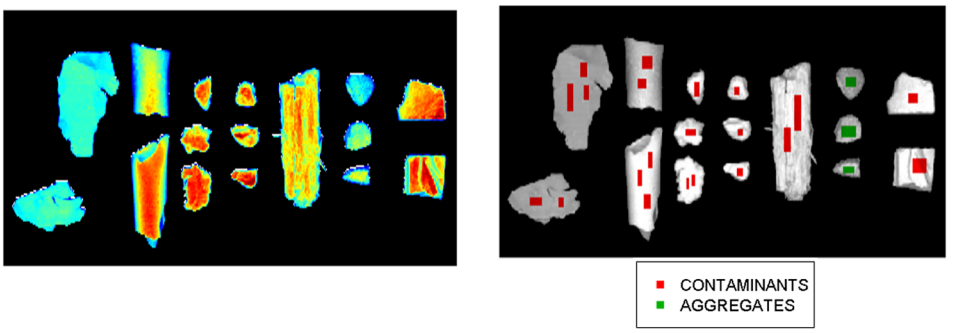

Fig. 4 Different classes of demolition waste (DW) materials. (a) Acquired hyperspectral image and (b) regions of interest (ROIs) selection for contaminant and aggregate classes.

Inc., Natick, Massachusetts) environment. A preliminary application of the preprocessing procedure was carried out in order to highlight differences between spectra corresponding to the different classes of material. Then principal components analysis (PCA) was applied in order to explore the data, to define classes and to evaluate the best algorithms for further classification models' development, setup, and implementation. The chosen method for classification and validation was the partial least-squares-discriminant analysis (PLS-DA).

3.1 *Preprocessing Step*

The background noise was eliminated by a preliminary reduction of the investigated wavelengths. At the beginning and at the end of the frequency field, wavelengths were cut, reducing spectral variables from 121 to 93: the corresponding new investigated wavelength interval was from 1006 to 1650 nm. The choice of wavelengths to be excluded was carried out after different experimental tests that showed what spectral variables give the noisiest signal. After this procedure, the background of each image was removed. Then data were preprocessed to highlight sample spectral differences and to reduce the impact of possible external sources of variability, allowing a more accurate interpretation of the classification model results.

Different preprocessing algorithms were applied: mean centering (MC), detrend and standard normal variate (SNV). MC is one of the most common preprocessing methods: it calculates the mean of each column and subtracts this from the column. It is useful to remove constant background contributions which usually are not interesting for the data variance interpretation.[17]

The detrend algorithm was applied to remove constant, linear or curved offsets. SNV is a weighted normalization and it was utilized to solve scaling, or gain effects, due to path length effects, scattering effects, source or detector variations, or other general instrumental sensitivity effects.[18]

3.2 *Exploratory Data Methods: Principal Component Analysis*

After preprocessing, an exploratory data analysis based on PCA was carried out.[19] PCA projects the samples into a low dimensional subspace whose axes are the principal components (PCs) pointing in the direction of maximum data variance in order to compress the data. PCA allows one to highlight the presence of trends or clusters among samples: according to the distribution of the samples on the PC space, it is possible to understand similarities and differences in their chemical/spectral behavior. Samples' grouping is an index belonging to the same class of materials that are characterized by similar spectral signatures.

3.3 *Classification Method: Partial Least-Squares-Discriminant Analysis*

PLS-DA is a linear classification method that combines the properties of partial least-squares regression with the discrimination power of a classification technique. PLS regression algorithm is the basis of PLS-DA: it looks for latent variables with a maximum covariance with the Y-variables.

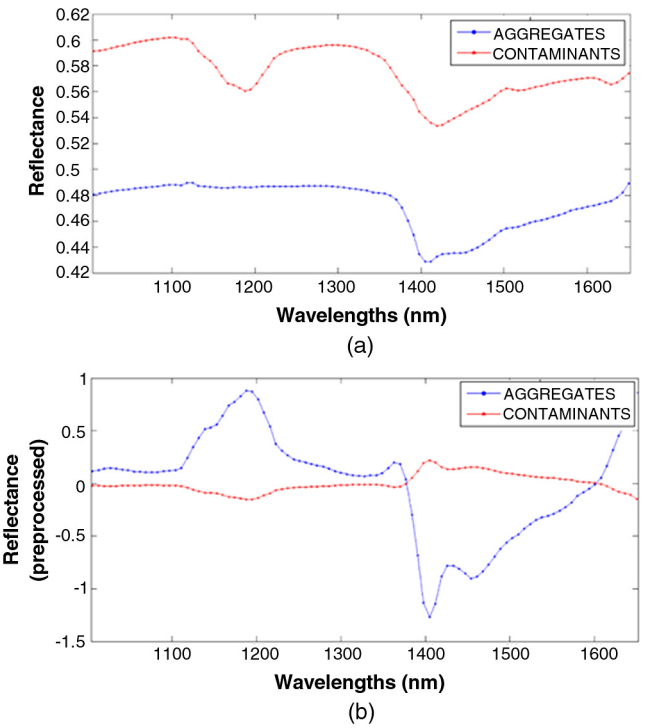

Fig. 5 (a) Raw spectra and (b) preprocessed spectra after the application of standard normal variate (SNV) and mean centering functions of aggregates and contaminants.

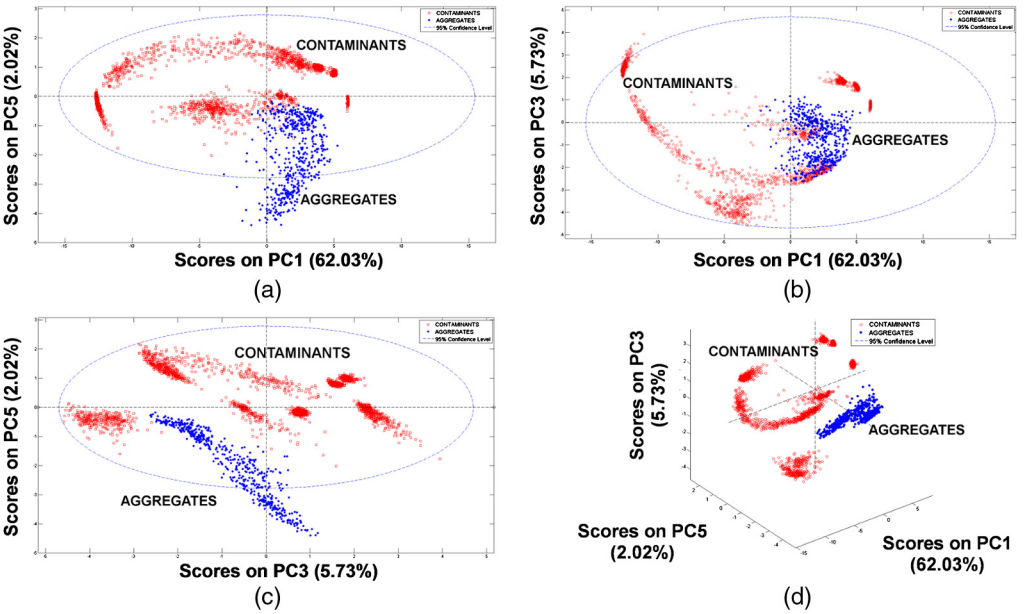

Fig. 6 Different combinations of P1-PC3-PC5 score plots showing the two classes of materials after the application of SNV and mean center preprocessing: (a) PC1 versus PC5, (b) PC1 versus PC3, (c) PC3 versus PC5 and (d) PC1 versus PC3 versus PC5.

In PLS-DA, the relevant sources of data variability are modeled by latent variables (LVs), which are linear combinations of the original variables: it allows graphical visualization and the understanding of the relations by LV scores and loadings. Scores represent the coordinates of a sample in the LVs' hyperspace, while loadings are the coefficients of variables in the linear combinations and they can be interpreted as the influence of each variable on each LV.[20] It is necessary to evaluate the optimal dimension of the LVs' subspace in order to perform the best classification model as possible.

PLS-DA is a supervised classification method;[21] therefore, it requires a prior knowledge of the data: a discriminant

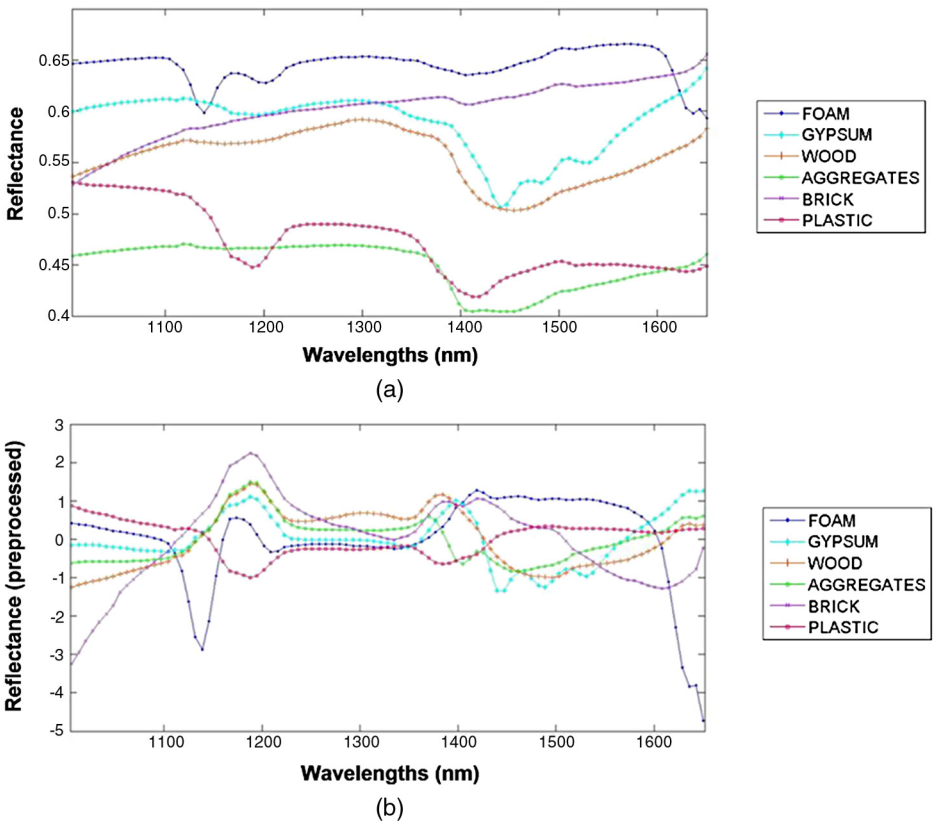

Fig. 7 (a) Acquired and (b) preprocessed spectra, resulting from Detrend, SNV, and mean center normalization algorithms application of the six different analyzed concrete contaminants.

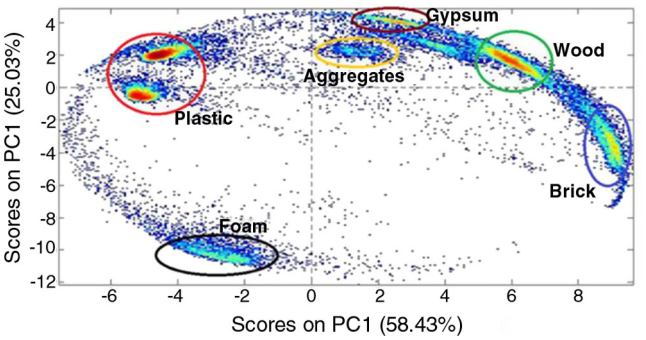

Fig. 8 PC1-PC2 score plot, obtained using 93 wavelengths, corresponding to the acquired image of six materials in the NIR field (1000–1700 nm). Detrend, SNV normalization, and mean centering (MC) were applied.

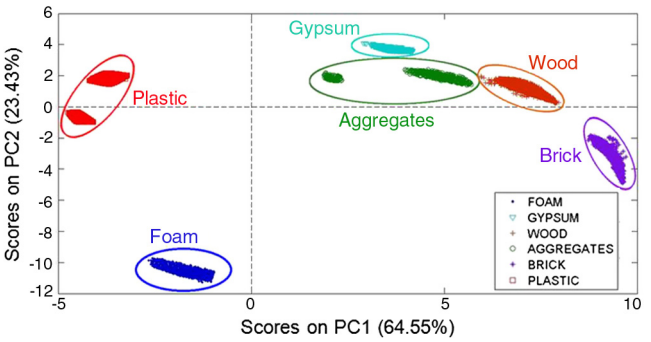

Fig. 9 PC1-PC2 score plot resulting after outlying pixels are removed from the training dataset in the NIR wavelength field (1000–1700 nm).

model is carried out using samples with known classes to be used later to classify new samples that are made of the same material as the known ones. Discriminant classification techniques look for what makes members of a class different from individuals in the other classes; as a consequence, these techniques operate by building models which assign one and only one of the categories represented in the dataset to each sample.[22] In particular, the PLS-DA method corresponds to the inverse-least-squares approach to linear discriminant analysis (LDA) and produces essentially the same results but with the noise reduction and variable selection advantages of PLS.[23]

In this study, PLS-DA was used to perform a good discrimination among classes of materials and to define predictions in new hyperspectral images, adopting preprocessing algorithms defined in the PCA step.

A class-modeling method such as soft independent modeling of class analogy is not useful in order to obtain the desired classification purpose because a different approach should be applied. In detail, this kind of technique concentrates on finding the similarity/analogies among individuals of the same class, rather than focusing on the differences between members belonging to different categories. Each category is independently modeled on the others and a sample can be assigned to only a class or even to more classes or can be rejected by all classes.

The obtained PLSDA model, instead, assigns only one of the available categories, based on its spectral signature, to each unknown sample in the hyperspectral image, making interpretation of the results easier. The results of PLS-DA, applied to hypercubes, are prediction maps, where each class is defined by a different color.

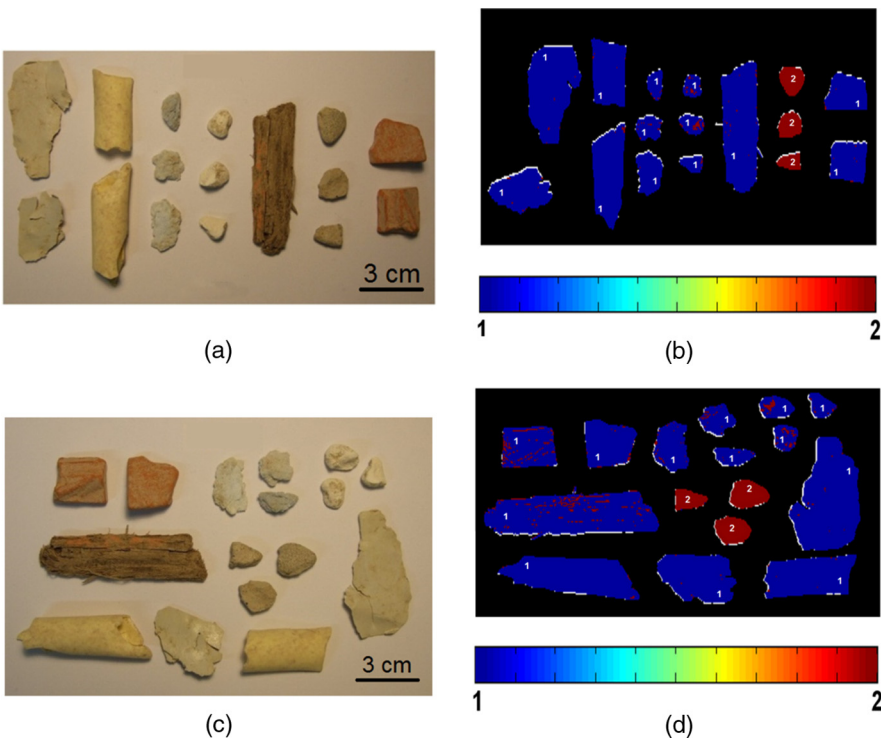

Fig. 10 (a and c) Source digital images set, (b) corresponding prediction images resulting from the application of the PLS-DA two classes' model to the same image utilized for training and (d) to the same particles topologically rearranged. Classes: (1) contaminants and (2) aggregates.

4 Results

The NIR range provides chemical information about the investigated materials, because most absorption bands observed in this interval arise from overtones of C-H, O-H, and N-H stretching vibrations. The interpretation of the results was addressed to verify the reliability and robustness of the proposed NIR-HSI procedures with respect to contaminants/aggregates recognition.

4.1 *Principal Component Analysis and Class Setting*

4.1.1 *Preliminary test: 2-classes model*

Different regions of interest (ROI) were selected in order to train the system to recognize the two classes of materials: aggregates and contaminants. Figure 4 shows the selected ROIs utilized for training dataset creation.

The original and the preprocessed average reflectance spectra of the two different classes are reported in Fig. 5. From the analysis of the spectra, it can be clearly outlined as the application of the preprocessing algorithms (SNV and mean center) highlights the differences among them.

Different combinations of PCs were plotted (Fig. 6). The analysis of the score plots clearly shows as the two different classes of products are recognized according to their grouping in a 3-D space formed by PC1, PC3, and PC5 [Fig. 6(d)]. PC1 and PC3 explained 62.03% and 5.73% of the variance, respectively while the PC5 explained 2.02%.

4.1.2 *Second experimental test: 6-classes model*

Collected spectra were preliminarily preprocessed. Detrend, SNV normalization, and MC were applied. In Fig. 7, raw and preprocessed spectra are reported. After preprocessing, PCA was then applied as exploratory data analysis. The analysis of the score plot allows one to identify six different groups according to material spectral signatures (Fig. 8). In this experimental setup, the majority of the variance was captured by the first two PCs, where PC1 and PC2 explained 58.43% and 25.03% of the variance, respectively. Some pixels of each identified group were selected in order to set classes and others were removed in order to build the training dataset for the following classification model. The training dataset was then analyzed by PCA again to better appreciate the reflectance differences between samples: similarities were expressed by sample grouping on the PCA score plot (Fig. 9). In this second case, the captured variance by PC1 increases up to 64.55%, explaining the majority of the sample variability.

4.2 *Partial Least-Square-Discriminant Analysis Classification*

The same algorithms used to perform the previous explorative analyses by PCA were applied to build PLS-DA models.

4.2.1 *Preliminary tests: 2-classes model*

The results achieved after the two classes' model application are shown in Fig. 10. The same image [Fig. 10(a)], adopted to realize the training dataset, was preliminarily classified and the results are shown in Fig. 10(b). The same particles were then spatially re-arranged [Fig. 10(c)] and their classification performed [Fig. 10(d)]. The built model was then applied to a new image containing samples not previously

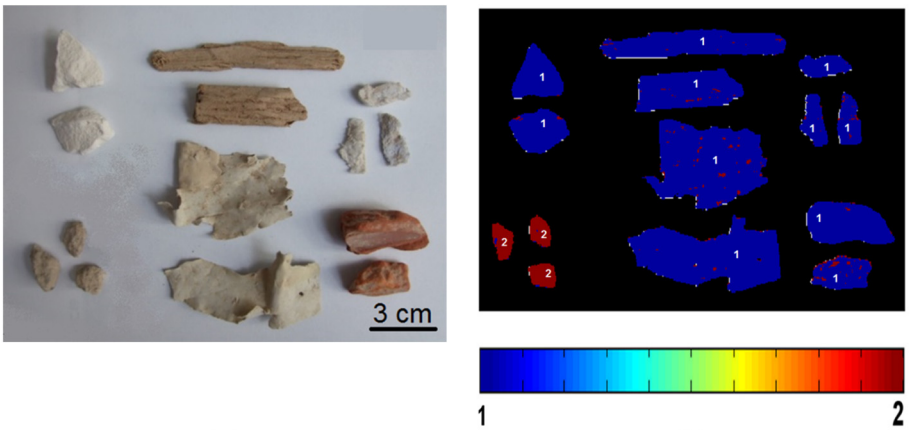

Fig. 11 (a) Source digital image set (b) and corresponding PLS-DA 2-classes model applied to a new image. Classes: (1) contaminants and (2) aggregates.

Table 2 Sensitivity and specificity values obtained for the two classes PLS-DA model built for aggregates and contaminants. Results are based on the modeling performed utilizing 93 wavelengths.

Applied algorithms in the PLS-DA model	Class	Sensitivity		Specificity	
		Calibration	Cross validation	Calibration	Cross validation
SNV and mean center	Contaminants	0.985	0.984	1.000	1.000
	Aggregates	1.000	1.000	0.985	0.984

Table 3 Sensitivity and specificity values obtained for the six classes' PLS-DA built for the different concrete contaminants, based on 93 wavelengths.

Applied algorithms in the PLS-DA model	Class	Sensitivity		Specificity	
		Calibration	Cross validation	Calibration	Cross validation
Detrend, SNV, mean center	Aggregates	0.941	0.947	0.995	0.896
	Brick	0.998	0.994	0.996	0.996
	Gypsum	0.983	0.983	0.999	0.999
	Plastic	1.000	1.000	1.000	1.000
	Wood	0.983	0.983	0.995	0.995
	Foam	1.000	1.000	1.000	1.000

utilized. The corresponding prediction map is shown in Fig. 11.

PLS-DA results can be better appreciated considering the values of the sensitivity and specificity obtained for each model. The sensitivity is a true positive rate: it is the estimation of the model's ability to avoid false negatives (i.e., number of samples of a given type correctly classified as that type). The specificity is the estimation of the model's ability to avoid false positives (the number of samples not of a given type correctly classified as not of that type). These values, ranging from 0 to 1, can give information about model efficiency: the higher the values are, the better the models are. The obtained values for the two classes' model are shown in Table 2.

From the analysis of the results showed in Figs. 10 and 11, it appears that in the 2-classes model, aggregates and contaminants are recognized. Even if some pixels are misclassified, the majority of them belong to the correct class in each object. These sporadic errors in prediction are probably due to the surface roughness of the sample, highlighting the scattering effect of the light, or to the presence of dirtiness on the sample surface.

4.2.2 *Second experimental test: 6-classes model*

The same images utilized to perform the preliminary test were then used to perform the six classes' modeling. The corresponding sensitivity and the specificity parameters are reported in Table 3.

Prediction maps of these images, used for validation, are shown in Figs. 12, 13, and 14. From the analysis of Figs. 12, 13, and 14, it can be noticed that good classification results were obtained. Some errors still occur between aggregates and brick, whereas aggregates are perfectly recognized with respect to the other classes of contaminants.

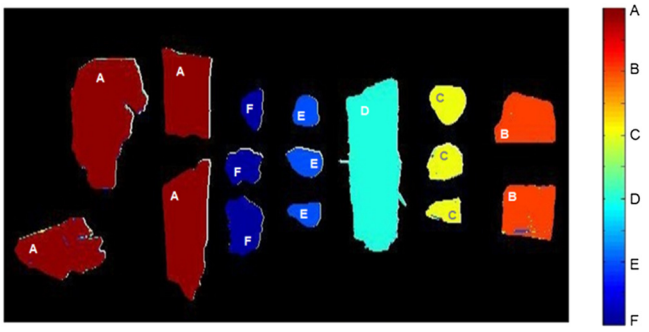

Fig. 12 PLS-DA six classes' model applied to the same image used to build the model. The classes are plastic (A), brick (B), aggregates (C), wood (D), gypsum (E) and foam (F).

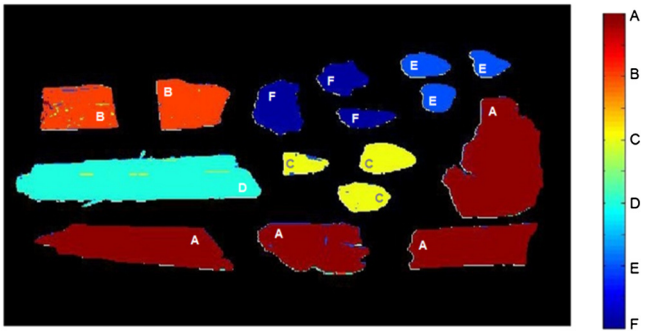

Fig. 13 PLS-DA six classes' model applied to the same particles used to build the model topologically rearranged. The classes are plastic (A), brick (B), aggregates (C), wood (D), gypsum (E) and foam (F).

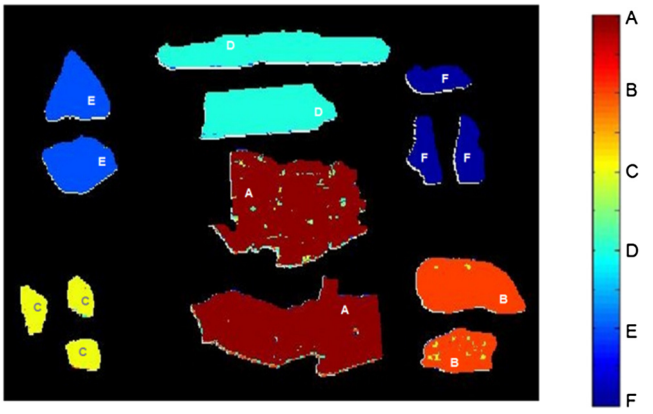

Fig. 14 PLS-DA six classes' model applied to a new image. The classes are plastic (A), brick (B), aggregates (C), wood (D), gypsum (E) and foam (F).

Some sporadic errors in brick and plastic classifications are visible, especially in the new image prediction map (Fig. 14). This phenomenon is probably due to the heterogeneity of investigated materials and, therefore, to the light scattering, but also to the "dirty" nature of this material as collected from a DW stream.

5 Conclusions

The use of HSI in the NIR range (1000–1700 nm) as a tool for recognition/classification of recycled aggregates and unwanted contaminants was investigated, developing different experimental setups.

Results showed that the proposed technology, combined with specific chemometric techniques, is particularly suitable to recognize the products obtained by a recycling process of DW in order to control the quality of the output streams. The results demonstrated that aggregates can be distinguished from concrete pollutants. A good recognition of all the different materials, both adopting the two classes' model and the six classes' model, is possible. Some few misclassifications in prediction occur, both for the two classes' and the six classes' models, probably due to the heterogeneity of samples or a border effect. Indeed, it is also important to take into account that these materials are not perfectly cleaned, so it is possible to have some impurities, characterized by their own spectral behavior, that negatively influence the recognition/classification process. In any case, it is important to note that this technique allowed us to recognize the presence of different materials inside a DW recycling plant, independently from some sporadic pixels misclassifications.

The proposed approach presents several advantages: it is objective, rapid, nondestructive, and low cost. This latter feature is really important in the secondary raw materials sector, where the utilization of expensive and/or sophisticated quality control devices cannot be practically proposed, both for technical (i.e., particles of different size, shape, and composition) and economic reasons.

Thus, the HSI based approach can be adopted to perform DW classification, which is useful for monitoring the concrete recycling process and to control its quality. This system could play a fundamental role in the DW recycling in the near future.

Acknowledgments

A special thanks is due to the European Commission for the financial support: this study was developed in the framework of the FP7 Collaborative project "Advanced Technologies for the Production of Cement and Clean Aggregates from Construction and Demolition Waste (C2CA)," Grant No. 265189.

References

1. F. Di Maio et al., "Cement and clean aggregates from CDW: the C2CA project," in *Proc. 27th Int. Conf. on Solid Waste Technology and Management*, 11–14 March 2012, 796–808, Widener University School of Engineering, Philadelphia, Pennsylvania (2012).
2. T. Hyvarinen, E. Herrala, and A. Dall'Ava, "Direct sight imaging spectrograph: a unique add-on component brings spectral imaging to industrial applications," *Proc. SPIE* **3302**, 165–175 (1998).
3. P. Geladi, H. Grahn, and J. Burger, "Multivariate images, hyperspectral imaging: background and equipment," in *Techniques and Applications of Hyperspectral Image Analysis*, H. Grahn and P. Geladi, Eds., pp. 1–15, John Wiley & Sons, West Sussex, England (2007).
4. P. Geladi, J. Burger, and T. Lestander, "Hyperspectral imaging: calibration problems and solutions," *Chemom. Intell. Lab. Syst.* **72**, 209–217 (2004).
5. A. Farcomeni, S. Serranti, and G. Bonifazi, "Non-parametric analysis of infrared spectra for recognition of glass and glass ceramic fragments in recycling plants," *Waste Manage.* **28**, 557–564 (2008).
6. G. Bonifazi and S. Serranti, "Hyperspectral imaging based techniques in fluff characterization," *Proc. SPIE* **6377**, 63770O (2006).
7. G. Bonifazi and S. Serranti, "Hyperspectral imaging based procedures applied to bottom ash characterization," *Proc. SPIE* **6755**, 67550B (2007).
8. G. Bonifazi et al., "Innovative recognition-sorting procedures applied to solid waste: the hyperspectral approach," [Sustainable development and planning IV], Book Series: *WIT Transactions on Ecology and the Environment*, C. A. Brebbia et al., Eds., Vol. **120**, pp. 885–894, WIT Press, Southampton, Boston (2009).
9. A. Dall'Ara, A. Bonoli, and S. Serranti, "An innovative procedure to characterize properties from tailored compost," *Environ. Eng. Manage. J.* **11**(10), 1825–1832 (2012).
10. B. Hu et al., "Recycling-oriented characterization of polyolefin packaging waste," *Waste Manage.* **33**, 574–584 (2013).
11. S. Serranti, A. Gargiulo, and G. Bonifazi, "Hyperspectral imaging for process and quality control in recycling plants of polyolefin flakes," *J. Near Infrared Spectrosc.* **20**, 573–581 (2012).
12. V. Luciani et al., "Quality control in the recycling stream of PVC from window frames by hyperspectral imaging," *Proc. SPIE* **8774**, 87741N (2013).
13. A. Ulrici et al., "Efficient chemometric strategies for PET-PLA discrimination in recycling plants using hyperspectral imaging," *Chemom. Intell. Lab. Syst.* **122**, 31–39 (2013).
14. G. Bonifazi and S. Serranti, "Hyperspectral imaging applied to end-of-life concrete recycling," *Proc. SPIE* **9022**, 90220V (2014).
15. R. Palmieri, G. Bonifazi, and S. Serranti, "Automatic detection and classification of EOL-concrete and resulting recovered products by hyperspectral imaging," *Proc. SPIE* **9106**, 91060D (2014).
16. S. Lotfi et al., "Mechanical recycling of EOL concrete into high-grade aggregates," *Resour. Conserv. Recycl.* **87**, 117–125 (2014).
17. R. Tauler et al., "Chemometrics modelling of environmental data," in *Proc. iEMSs 2004 Int. Congress: "Complexity and Integrated Resources Management*," International Environmental Modelling and Software Society, Osnabrueck, Germany (2004).
18. B. M. Wise et al., *Chemometrics Tutorial for PLS_Toolbox and Solo*, Eigenvector Research, Inc., 3905 West Eaglerock Drive, Wenatchee, Washington (2007).
19. S. Wold, K. Esbensen, and P. Geladi, "Principal component analysis," *Chemom. Intell. Lab. Syst.* **2**, 37–52 (1987).
20. D. Ballabio and V. Consonni, "Classification tools in chemistry. Part 1: linear models.PLS-DA," *Anal. Methods* **5**, 3790–3798 (2013).
21. M. Barker and W. Rayens, "Partial least squares for discrimination," *J. Chemom.* **17**, 166–173 (2003).
22. A. Biancolillo et al., "Data-fusion for multiplatform characterization of an Italian craft beer aimed at its authentication," *Anal. Chim. Acta* **820**, 23–31 (2014).
23. D. Ballabio and R. Tedeschini, "Multivariate classification for qualitative analysis," in *Infrared Spectroscopy for Food Quality Analysis and Control*, S. Da-Wen, Ed., pp. 83–104, Academic Press/Elsevier, London, UK, (2009).

Silvia Serranti is an associated professor at the Department of Chemical Materials Environment Engineering (DICMA) at La Sapienza–University of Rome. She is a PhD geologist and worked for 15 years in the Raw Materials Unit of DICMA. Her research activity is related to primary and secondary raw materials' characterization and valorization, documented by more than 100 scientific papers in international journals and conference proceedings, and participating in 12 European research projects in European.

Roberta Palmieri is a PhD student at La Sapienza–University of Rome in electrical engineering, materials, and nanotechnology. She graduated with honors in environmental engineering at La Sapienza in 2013 and started her PhD career in the same year. Most of her current PhD research is about raw materials and secondary raw materials characterization, using classical and innovative approaches, in particular hyperspectral imaging analysis.

Giuseppe Bonifazi is a full professor of raw materials beneficiation at the DICMA at La Sapienza–University of Rome. He has more than 30 years of experience on particles and particulate solids characterization. His main research fields are related to the study of software and hardware architectures for the synthesis, classification, and recognition of numeric signals, and development and setup of procedures for materials identification using multi- and hyperspectral imaging techniques.